电子束焊 GH4169合金高温裂纹尖端张开位移试验

吴 冰[1], 左从进[1], 李晋炜[1], 张彦华[2], 熊林玉[2]

(1. 北京航空制造工程研究所, 北京 100024
2. 北京航空航天大学 机械学院, 北京 100083)

吴 冰

摘 要: 根据国标 GB/T 2358-94 对 GH4169合金电子束焊接接头的高温(650℃)裂纹尖端张开位移(CTOD)进行了测试。取 SE(B)试样进行三点弯曲试验, 然后由所得到的650℃下母材和焊缝的 $P-V$ 曲线来计算 CTOD值, 并对试验结果进行了讨论和总结。

关键词: 电子束焊接; GH4169合金; 高温; 裂纹尖端张开位移;
中图分类号: TG456.3 文献标识码: A 文章编号: 0253-360X(2005)11-109-04

0 序 言

电子束焊接(简称 EBW)技术以其高能量密度、高熔透性、焊接变形区小及易于控制等优点在航空领域得到广泛的应用。在 20世纪 80年代, 西方国家研制的高水平、高性能飞机及其发动机的特点是越来越多地采用焊接结构, 其中电子束焊接已广泛应用于飞机的重要受力构件和发动机部件。

GH4169合金作为航空发动机制造中的主要材料, 应用于发动机的高温部件。由于常常处在高温等恶劣的环境下服役, 所以良好的高温韧性是保证管道安全运行的重要因素之一。CTOD(裂纹尖端张开位移)断裂韧度是评价材料及焊接接头抗脆断特性的重要参量。与传统的夏比 V形缺口冲击韧度比较, CTOD更能有效准确地评价钢材的抗脆断能力。通过 CTOD试验不仅可以进行材料韧度选择, 还可以为评定结构的安全可靠性提供试验依据[1,2]。

近年来, 采用电子束焊接 GH4169合金材料的发动机构件的比重越来越大。因此, 作者对电子束焊 GH4169合金高温裂纹尖端张开位移 CTOD试验进行研究具有重要意义。

1 试样制备

试验采用的材料为 GH4169合金。基材的化学成分见表 1[3], 650℃温度下 GH4169合金母材及电子束焊缝力学性能见表 2。电子束焊缝经 X射线检测无缺陷。

根据国家标准GB/T2358-94[4], 制备带预制疲劳裂纹的直三点弯曲 SE(B)试样, 标准 SE(B)试样见图 1。试验需制备母材 SE(B)试样 3件, 带电子束焊缝 SE(B)试样 3件, 各试样的几何尺寸列于表 3中。

表 1 GH4169合金化学成分(质量分数, %)
Table 1 Chemical composition of GH4169

C	Cr	Ni	Co	Mo	Al	Ti	Fe	Nb
≤0.08	17.0~21.0	50.0~55.0	≤1.0	2.80~3.30	0.30~0.70	0.75~1.15	余	4.75~5.50
B	Mg	Mn	Si	P	S	Cu	Ca	Pb	Se
≤0.006	≤0.01	≤0.35	≤0.35	≤0.015	≤0.015	≤0.30	≤0.01	≤0.0005	≤0.0003

预制疲劳裂纹。根据国标 GB/T2358-94, 所有试样必须通过疲劳的方法产生预裂纹, 疲劳引发裂纹时采用的最大疲劳载荷 $p_{f\max}$ 应不大于 p_f。

$$p_f = 0.5Bb_0^2\sigma_Y / S。 \quad (1)$$

式中: B 为试验厚度; b_0 为原始韧带; S 为弯曲试样加载跨距; σ_Y 为有效屈服强度。

收稿日期: 2005-09-21

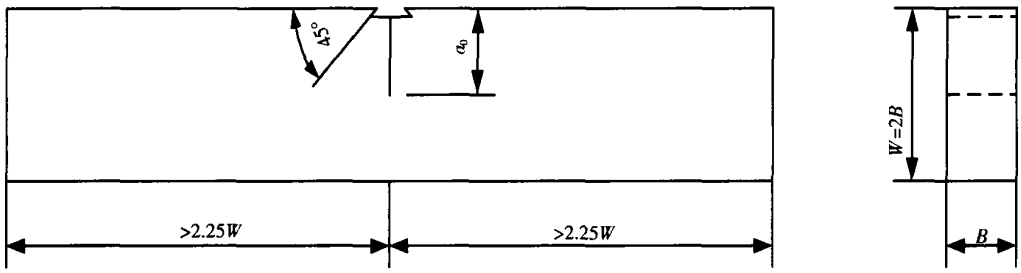

图 1 直三点弯曲 SE(B)试样

Fig. 1 Three point bend specimen

表 2 GH4169合金母材及电子束焊缝力学性能

Table 2 Mechanical properties of GH4169

加热温度 T/℃	取样位置	屈服强度 $\sigma_{0.2}$/MPa	弹性模量 E/GPa	泊松比 μ
650	母材	1 075	133	0.325
	电子束焊缝	1 009	127	0.325

表 3 试样几何尺寸

Table 3 Geometrical dimension of specimens

试样序号	取样位置	试验温度 T/℃	厚度 B/mm	宽度 W/mm
M_1	母材	650	15.06	30.10
M_2			15.06	30.08
M_3			15.06	30.12
H_1	电子束焊缝	650	15.01	30.09
H_2			15.01	30.12
H_3			15.01	30.09

SE(B)试样, 对于母材试样, 疲劳裂纹的取向为 $L-T$, 即裂纹面垂直于轧制方向; 对于电子束焊缝试样, 焊接方向垂直于轧制方向, 疲劳裂纹沿焊缝方向开, 其疲劳裂纹取向为 $L-T$. 在此需要说明一点, 电子束焊缝宽度较窄, 热影响区的宽度更是有限, 在热影响区预制疲劳裂纹无法实现, 因此试验只在焊缝中心预制疲劳裂纹。

2 试验程序

在试验温度下对载荷、位移测量系统进行标定, 在连续做试验之前, 也要对载荷、位移测量系统进行标定。

2.1 试验步骤

(1) 在 MTS 810.13试验机上进行 CTOD试验。

(2) 将试验件装夹在试验机上, 将试件放在炉子中加热至 650 ℃后进行保温。

(3) 采用一次加载方式直到试件失稳, 加载速率控制在 1 mm/min范围内, 并同时记录试样载荷位移曲线。

2.2 数据处理

(1) 根据国标 GB/T 2358-94, 取脆性失稳断裂点或突进点所对应的特征载荷 p与位移 V计算 δ

(2) δ的计算方法。获得必要的测量数据后, 采用下列公式计算原始裂纹尖端部位的张开位移

$$\delta=\frac{K_1^2(1-\mu^2)}{2\sigma_y E}+\frac{r_p(W-a_0)V_p}{r_p(W-a_0)+a_0+Z} \tag{2}$$

式中: μ为泊松比; σ_y为被测材料在试验环境下的屈服强度; E为被测材料在试验环境下的弹性模量; r_p为塑性转动因子, 对于三点弯曲试样, $r_p=0.44$; V_p为 $P-V$曲线上取值点对应的夹式引伸计张开位移的塑性部分; K_1为根据取值点载荷计算的Ⅰ型应力强度因子; W为试样宽度; a_0为原始裂纹长度; Z为引伸计装夹部位到试样表面的距离即刀口厚度。

$$K_1=\frac{YP}{BW^{1/2}} \tag{3}$$

式中: Y为试样几何形状因子。

对于直三点弯曲试样, $0.45\leqslant a_0/W\leqslant 0.55$

$$Y=\frac{6(\frac{a_0}{W})^{1/2}\{1.99-\frac{a_0}{W}(1-\frac{a_0}{W})[2.15-3.93\frac{a_0}{W}+2.7(\frac{a_0}{W})^2]\}}{(1+2\frac{a_0}{W})(1-\frac{a_0}{W})^{3/2}}\cdot\frac{S}{4W} \tag{4}$$

3　试验结果及分析

3.1　试验结果

试验测得的典型载荷 -位移曲线见图 2。典型试样的宏观断口形貌见图 3。650 ℃母材、焊缝计算结果见表 4。

3.2　试验结果分析

由表 4可以看出,在 650 ℃温度下,GH4169合金母材的 CTOD值比 EBW焊缝的 CTOD值高。试验中母材和焊缝分别做了 3个试样,3个试样的 CTOD平均值为母材 $\delta_M = 0.1102$ mm。

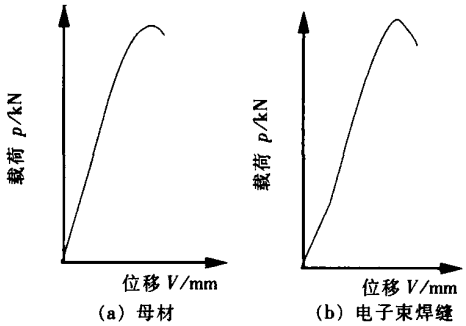

图 2　典型载荷 -位移曲线

Fig. 2　Typical curve of force vs displacement

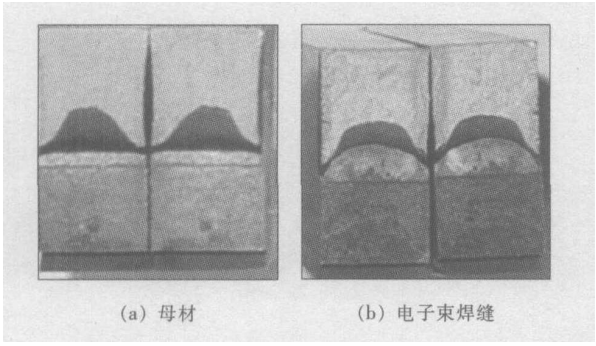

图 3　典型试样的宏观断口形貌

Fig. 3　Typical fracture appearance of specimens

EBW焊缝 $\delta_H = 0.0698$ mm,$\delta_M - \delta_H = 0.0404$ mm,EBW焊缝与母材相比 CTOD值下降较多。此结果说明,EBW焊缝的断裂韧度比母材的差,也就是说经电子束焊接后,材料变脆,其抗脆断能力比母材差。

表 4中 CTOD值是通过式(2)、(3)、(4)计算得到的,式(2)包括两项,可表示为 $\delta = S + T$,其中:

$$S = \frac{K_1^2(1-\mu^2)}{2\sigma_y E}, \tag{5}$$

$$T = \frac{r_p(W-a_0)V_p}{r_p(W-a_0)+a_0+Z}。 \tag{6}$$

各试样 S、T计算值见表 5。从表 5可以看出,各试件的 S值相差不多,而试件 M_1、M_2、M_3的 T值要比 H_1、H_2、H_3的 T值高很多,最终影响母材和焊缝 CTOD值的项是 T项。式(6)中,r_p是常数 0.44,各个试件的 W和 a_0项差不多,那么只有 V_p对 T项的大小起决定性作用。因此,从以上的分析可得到,此次试验中,各个试件 V_p值是决定 CTOD值的大小主要因素。V_p表示引伸计张开位移的塑性分量,那么可以得到这样的结论,对于此次试验,试样的塑性位移决定着材料的抗脆断能力。

表 4　650 ℃温度下 CTOD试验计算结果

Table 4　Calculated results of CTOD at 650 ℃

试样编号	试样状态	原始裂纹长度 a_0/mm	试验载荷 p/kN	引伸计张开位移 V_p/mm	特征 CTOD δ/mm
M_1	母材	14.65	36.82	0.202 92	0.129 1
M_2		14.84	33.50	0.131 46	0.096 9
M_3		15.03	34.76	0.138 35	0.104 7
H_1	电子束焊缝	15.75	31.21	0.052 15	0.081 1
H_2		17.01	24.29	0.035 54	0.062 2
H_3		17.26	24.19	0.039 44	0.066 0

表 5　各试样 S、T计算值

Table 5　Calculated results of S and T in Exp. 2

试样编号	S/mm	T/mm
M_1	0.064 8	0.064 3
M_2	0.055 9	0.040 9
M_3	0.062 3	0.042 4
H_1	0.066 2	0.014 9
H_2	0.053 2	0.009 0
H_3	0.056 3	0.009 7

4　结　　论

(1) 从试验结果可以看出,CTOD值由高到低的顺序为母材>焊缝。因此,母材的高温断裂韧度较焊缝好。

(2) 经分析可知,对于此次试验,引伸计张开位

移的塑性分量 V_p 对材料的抗脆断性能起着决定性作用。

参考文献:

[1] 霍立兴. 焊接结构工程强度[M]. 北京: 机械工业出版社, 1995. 68 – 89.
[2] 霍立兴. 焊接结构的断裂行为及评定[M]. 北京: 机械工业出版社, 2000. 46 – 77.
[3] 《中国航空材料手册》编辑委员会. 中国航空材料手册(第 2卷)[M]. 北京: 中国标准出版社, 2001. 323 – 360.
[4] GB/T 2358 – 94. 金属材料裂纹尖端张开位移试验方法[S].

作者简介: 吴 冰, 女, 1978年 8月出生, 硕士研究生, 助理工程师。研究方向为电子束焊接, 发表论文 4篇。

Email: alice. bing@163. com

status of joint were evidently affected by changing of h_s (i. e. beam offset on steel side), a small quantity of metal QCr0. 8 melted down into weld as value of h_s was less, a large difference of microstructures and chemical composition existed in comparison of weld with base metal QCr0. 8. With increasing of h_s the microstructure distribution of joint becomes homogeneous gradually, but the bad fusion's status happened to QCr0. 8 side in weld due to unbalanced heat input and rapid heat conduction of QCr0. 8. Even if h_s increased in little range, base metal QCr0. 8 may not be fusion, which resulted in forming joint of local fusion or lack of fusion.

Key words: electron beam welding; microstructure; phase composition

Hydrogen behavior in titanium alloy EBW joints WANG Ya-jun[1,2], TANG Xiao-qing[1], LIU Hao[2], GUAN Qiao[2] (1. Beijing hangkong university, Beijing 100083, China; 2. Beijing aeronautical manufacture technology research institute. Beijing 100024, China). p93 - 96

Abstract: The electrolytic hydrogen charging with constant current and X - ray diffraction were used to investigate the hydrogen content threshold of the hydrogen induced cracking for Ti1023 titanium alloy EBM joints and the effect of the microstructure phase on sensitivity of hydrogen induced cracking. The scanning electronic microscopy was employed to observe the fracture appearance on different hydrogen charging condition. By means of the artificial aging and ion probe analysis, the dynamic behavior of hydrogen in Ti1023 titanium alloy EBM joints was also studied in this paper.

Key words: Ti1023 titanium alloy; EBM; hydrogen induced cracking

Application of fuzzy-PID control on seam tracking for welding-robot YE Jian-xiong, ZHANG Hua (school of Mechanical and Electronic Engineering, Nanchang University, Nanchang 330029, China). p97 - 100

Abstract: A convenient and effective close loop control scheme, had been proposed to satisfy the aim of seam tracking based on the analysis of the welding-robot modeling and its control link in this paper. With the introduction of fuzzy controller and PID controller and with the adoption of the simulation on the differentiated modeling, the characteristics of the hybrid manipulator were illuminated. In the end, some conclusions were drawn on the base of analysis of the different response curves.

Key words: fuzzy; PID; hybrid-manipulator; self-adaptation; simulation

Ultrasonic signal analyses of spot welds in thin steel sheet ZHAO Xin-yu, GANG Tie, YUAN Yuan (State key Laboratory of Advanced Welding Production Technology, Harbin Institute of Technology, Harbin 150001, China). p101 - 105

Abstract: The quality of spot welds in galvanized sheet metal was evaluated by using ultrasonic water immersion focusing method. The A-scan signal, B- and C-scan image features of spot welds were analyzed. The feasibility of evaluating the quality of spot welds by using the B-scan image was provided. By using the method, not only the kiss bonding and the perfect joint could be evaluated qualitatively, but also the pressure mark depth of the upper-bottom surface and the spot weld diameter could be calculated quantitatively. The accuracy of testing result was verified by contrasting the metallographs of actual spot welds cross section.

Key words: ultrasonic test; water immersion focusing; resistance spot weld

Comparison of fatigue property for TIG welding of TC4 and TA15 tianium alloy WANG Xiang-ming (Shenyang Aircraft Design & Research Institute, Shenyang 110035, China). p106 - 108

Abstract: As the researched objects, TIG welded test specimens of titanium TC4 and TA15 were selected, and their fatigue tests were done under different constant amplitude spectrums with four stress levels, respectively. According to the contrast analysis for the fatigue test results by use of three-parameter-model of fatigue life founded in this paper, the fatigue property of TA15 TIG weld was better than TC4 TIG weld appreciably in $10^4 \sim 10^6$ region. The possible affected factors were discussed.

Key words: Titanium; weld; fatigue

Experimeneal research on high Temperature CTOD of electron beam welded joints of GH4169 alloy WU Bing[1], ZUO Cong-jin[1], LI Jin-wei[1], ZHANG Yan-hua[2], XIONG Lin-yu[2] (1. BAMTRI, Key laboratory for high energy density beam processing technology, Beijing 100024, China; 2. Beijing University of Aeronautics and Astronautics, Beijing 100083, China). p109 - 112

Abstract: In accordance with GB/T 2358-94, CTOD (crack-tip opening diaplacement) tests were conducted at 650 ℃ for electron beam welded joints of GH4169 alloy. According to the requirements of the standard, the specimen was a standard SE(B) (three point bending), the results were calculated using the P-V curves of parent material and weld metal. Finally, the test results were summarized and analysed.

Key words: electron beam welding; GH4169; high temperature; CTOD